

Mechanisms of elevated-temperature deformation in the B2 aluminides NiAl and CoAl

D. L. YANEY

Lockheed Missiles and Space Company Inc., Research and Development Division, 0/93-10, B/204, 3251 Hanover Street, Palo Alto, California 94304, USA

W. D. NIX

Department of Materials Science and Engineering, Stanford University, Stanford, California 94305, USA

A strain rate change technique, developed previously for distinguishing between pure-metal and alloy-type creep behaviour, was used to study the elevated-temperature deformation behaviour of the intermetallic compounds NiAl and CoAl. Tests on NiAl were conducted at temperatures between 1100 and 1300 K while tests on CoAl were performed at temperatures ranging from 1200 to 1400 K. NiAl exhibits pure-metal type behaviour over the entire temperature range studied. CoAl, however, undergoes a transition from pure-metal to alloy-type deformation behaviour as the temperature is decreased from 1400 to 1200 K. Slip appears to be inherently more difficult in CoAl than in NiAl, with lattice friction effects limiting the mobility of dislocations at a much higher temperature in CoAl than in NiAl. The superior strength of CoAl at elevated temperatures may therefore be related to a greater lattice friction strengthening effect in CoAl than in NiAl.

1. Introduction

Ordered intermetallic compounds have long been of interest as potential structural materials for use at elevated temperatures. In particular, the B2 aluminides NiAl and CoAl have received considerable attention in recent years. Both compounds exist over a range of compositions and, as summarized in Table I, have extremely high melting points [1], high stiffnesses [2], reasonably low densities [3] and the potential for self-protection in oxidizing atmospheres. Despite these similarities, however, the strength of CoAl is noticeably superior to that of NiAl [4-6]. Fig. 1 shows the difference in compressive flow strength between NiAl and CoAl over a range of compositions at 1300 K. The data are those of Whittenberger [4, 5], interpolated for a strain rate of $1 \times 10^{-4} \text{ sec}^{-1}$. The decrease in strength observed in CoAl with increasing deviation from stoichiometry has also been observed in NiAl at slightly higher temperatures [7] and is thought to be related in both cases to an increase in point-defect concentration with increasing deviation from the equiatomic composition [8]. Despite the ability of point defects to alter the strength of B2 compounds, Fig. 1 clearly shows that CoAl is significantly stronger than NiAl over a wide range of compositions. However, it is important to realize that the superior strength of CoAl at 1300 K is not related to a difference in stiffness and/or to a difference in diffusivity between NiAl and CoAl. At high homologous temperatures, the activation energy for deformation in many materials is approximately equal to the activation energy for lattice self-diffusion. Since this implies that strain rate is linearly proportional to diffusivity, a large difference

in lattice diffusivity between NiAl and CoAl at 1300 K could explain the difference in strength between these two compounds. However, as noted by Hocking *et al.* [6], for alloys of the stoichiometric composition, the rate of diffusion of ^{60}Co is only approximately two times faster in NiAl than in CoAl. Assuming that a power-law relationship of the form $\dot{\epsilon} = A\sigma^5$ adequately describes deformation under steady-state conditions in both NiAl and CoAl, it can be seen that a factor of two difference in strain rate is related to only a factor of 1.15 difference in stress. Thus, differences in diffusivity cannot account for the difference in elevated-temperature strength between stoichiometric NiAl and CoAl.

In addition to differences in diffusivity, large differences in stiffness could also explain the superior strength of CoAl at 1300 K. It is well known that the decrease in stiffness which typically accompanies an increase in temperature in most materials results directly in a decrease in elevated-temperature strength. Thus, if the stiffness of NiAl were considerably less than that of CoAl at 1300 K, the difference in strength between these two compounds could be easily understood. However, this is not the case. Harmouche and Wolfenden [2] report a value of 215 GPa for the Young's modulus of equiatomic CoAl at 1300 K. These authors also determined the modulus of equiatomic NiAl, although only at room temperature. However, if the linear decrease in Young's modulus with increasing temperature of 0.033 GPa K^{-1} reported by Rusovic and Warlimont [9] for equiatomic NiAl is used to correct the room-temperature modulus of Harmouche *et al.* [2], a Young's modulus of 195 GPa

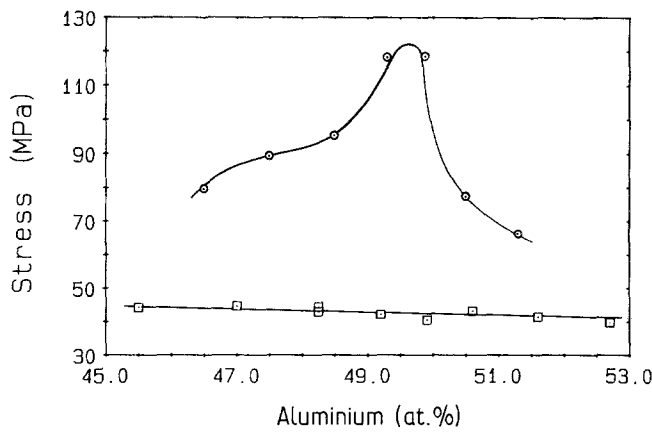


Figure 1 Compressive flow strength as a function of composition for (□) NiAl [4] and (○) CoAl [5] tested at 1300 K. Strain rate $1 \times 10^{-4} \text{ sec}^{-1}$.

is calculated for NiAl at 1300 K. Thus, neither differences in stiffness nor differences in diffusivity can be used to explain the difference in elevated-temperature strength between CoAl and NiAl.

As a first step toward understanding the factors that control deformation in CoAl and NiAl, Yaney *et al.* [10] identified the slip systems that operate in CoAl during extrusion at 1505 K and compared their findings with the results of similar investigations on NiAl. As reviewed by these authors, considerable information currently exists in the open literature regarding slip systems in NiAl. This information is summarized in Table II. Numerous single-crystal deformation studies have clearly shown that the ease of slip in NiAl is strongly dependent on crystal orientation. For crystals in which the deformation axis is not aligned with an $\langle 001 \rangle$ crystal direction, slip occurs fairly easily. Regardless of temperature, slip occurs preferentially along $\langle 001 \rangle$ directions, primarily on $\{100\}$ - and $\{110\}$ -type planes. When the deformation axis is aligned with an $\langle 001 \rangle$ crystal direction, however, $\langle 001 \rangle$ slip is prevented and plastic flow is much more difficult. In fact, Ball and Smallman [11] have shown that NiAl crystals oriented to prevent $\langle 001 \rangle$ slip (compression axis parallel to $\langle 001 \rangle$) are 20 times stronger at 823 K than crystals oriented to allow $\langle 001 \rangle$ slip (compression axis parallel to $\langle 011 \rangle$). Below approximately $0.45T_m$, crystals oriented to prevent $\langle 001 \rangle$ slip deform by the motion of $b = \langle 111 \rangle$ dislocations, reportedly on a variety of slip planes. Thus, $\langle 111 \rangle$ slip is more difficult than $\langle 100 \rangle$ slip. At higher temperatures, $\langle 111 \rangle$ slip is joined by $\langle 110 \rangle$ slip, with the frequency of $\langle 110 \rangle \{1\bar{1}0\}$ slip increasing with increasing temperature [12]. Apparently $\langle 110 \rangle$ slip is intrinsically more difficult than either $\langle 111 \rangle$ or $\langle 100 \rangle$ slip.

With respect to slip in CoAl, Yaney *et al.* [10], using diffraction contrast analysis, showed that $b = \langle 100 \rangle$

as well as $b = \langle 111 \rangle$ dislocations contribute to deformation of a Co-49.3 at % Al alloy during extrusion at 1505 K ($0.78T_m$). Thus, as in NiAl, sufficient slip systems exist in CoAl to allow for general plasticity in the absence of diffusional mechanisms. However, the fact that $b = \langle 110 \rangle$ dislocations were not observed in that investigation, despite the relatively high extrusion temperature, suggests that activation of the $\langle 110 \rangle \{1\bar{1}0\}$ slip system may be even more difficult in CoAl than in NiAl.

From the information outlined above it is apparent that the stress required to produce dislocation glide in NiAl (and presumably CoAl) is significantly greater for some slip systems than for others. In other words, lattice friction effects may limit the glide mobility of dislocations on certain slip systems in these intermetallics. Although it is often assumed that the only way to cause dislocations to move in a viscous manner is through the introduction into the matrix of appropriate solute atoms, it is important to realize that lattice friction effects may also reduce the glide mobility of dislocations. Recall that lattice friction effects are quite important in such covalently bonded solids as germanium and silicon [13, 14] in which the bonding is highly directional. Thus, it is not unreasonable to postulate that lattice friction effects may also be important in ordered intermetallic compounds in which strong repulsive forces exist between atoms of like character. The deformation behaviour of B2 compounds in which lattice friction effects limit the glide mobility of dislocations may be quite similar to the deformation behaviour of Class I solid-solution alloys in which solute atoms act to impede dislocation motion.

In this investigation, a strain rate change technique, developed previously [15] for distinguishing between

TABLE I Selected properties of NiAl and CoAl

Material	Property		
	Melting point (K) [1]	Young's modulus at room temperature (GPa) [2]	Density at room temperature (g cm^{-3}) [3]
NiAl	1913	230	5.85
CoAl	1921	296	6.07

TABLE II Operative slip systems in NiAl

Temperature	Orientation*	
	"Soft"	"Hard"
$T < 0.45T_m$	$\langle 100 \rangle \{001\}$	$\langle 111 \rangle \{\bar{1}\bar{1}2\}$
	$\langle 100 \rangle \{011\}$	$\langle 111 \rangle \{1\bar{1}0\}$
	$\langle 100 \rangle \{012\}$	$\langle 111 \rangle \{2\bar{1}3\}$
$T > 0.45T_m$	$\langle 100 \rangle \{001\}$	$\langle 110 \rangle \{1\bar{1}0\}$
	$\langle 100 \rangle \{011\}$	$\langle 111 \rangle \{\bar{1}\bar{1}2\}$

*"Soft" orientation: axis of deformation away from $\langle 001 \rangle$.

"Hard" orientation: axis of deformation near $\langle 001 \rangle$.

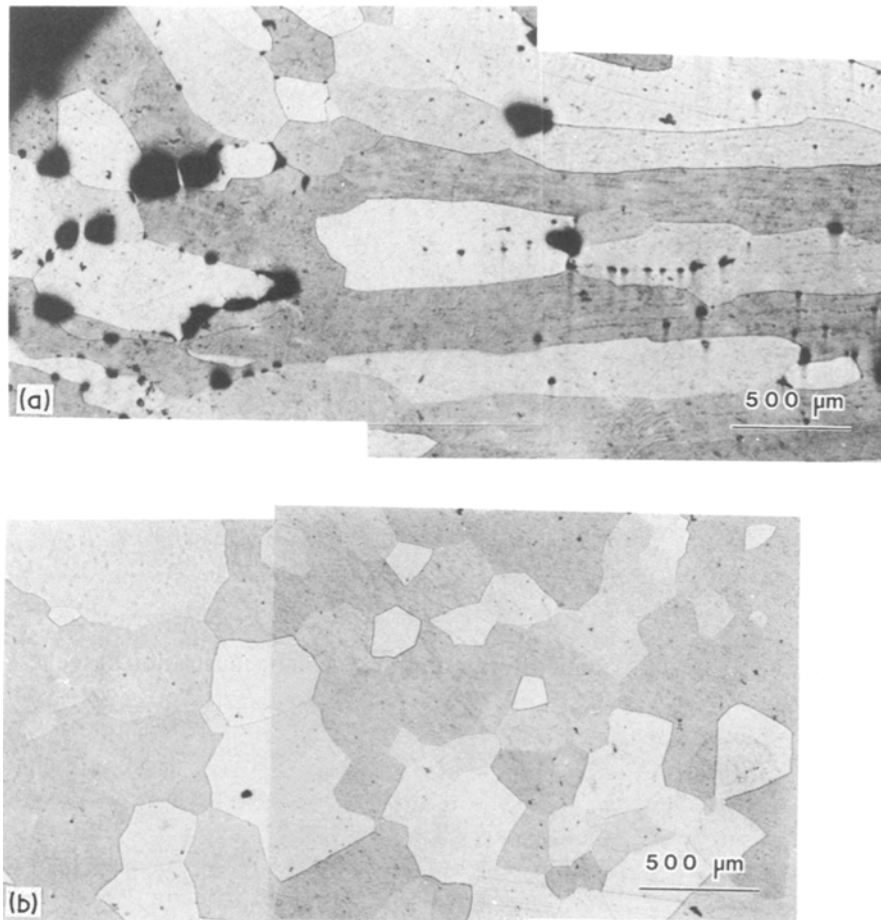


Figure 2 Optical micrograph of as-cast Ni-49.3 at % Al sectioned (a) perpendicular and (b) parallel to the length of the casting. Etched with a solution containing equal parts by volume of HCl, HNO₃ and CH₃COOH.

pure-metal and alloy types of creep behaviour, was used to determine if lattice friction effects limit the glide mobility of dislocations in either NiAl or CoAl. The results of strain rate change experiments performed on NiAl and CoAl are presented below and shown to be consistent with the observed difference in strength between these two materials at elevated temperatures.

2. Experimental procedures

2.1. Materials and sample preparation

In this investigation, two types of NiAl were tested: (i) at 49.3 at % Al alloy prepared by conventional casting techniques and (ii) a 48.2 at % Al alloy consolidated by the extrusion of pre-alloyed powders. The 49.3 at % Al alloy was obtained from the Oak Ridge National Laboratory in the form of a cylindrical casting approximately 12.7 mm (0.5 in.) in diameter and 102 mm (4 in.) in length. Compression specimens 5.08 mm (0.2 in.) in diameter and 10.2 mm (0.4 in.) in length were electro-discharge-machined from the casting with the compression axis parallel to the length of the casting. As can be seen in Fig. 2, the grains in the as-cast alloy were fairly large and non-equiaxed.

Cylindrical compression specimens of the Ni-48.2 at % Al alloy were supplied by the NASA Lewis Research Center. These specimens were 5.08 mm (0.2 in.) in diameter and varied in length from 7.6 mm (0.3 in.) to 10.2 mm (0.4 in.). As noted above, this alloy was prepared by powder metallurgy techniques. Gas-atomized powders of the 48.2 at % Al composition were consolidated by extrusion at 1505 K using a 16:1 reduction. After extrusion, Whittenberger [4] noted

that the alloy contained 0.4 vol % oxides in the form of stringers parallel to the extrusion axis. Consolidation produced equiaxed grains approximately 18 μm in diameter.

Cylindrical compression specimens of the Co-49.3 at % Al alloy tested in this investigation were also provided by the NASA Lewis Research Center. Dimensions for these specimens are as described previously for the Ni-48.2 at % Al alloy. As discussed by Whittenberger [5], the Co-49.3 at % Al alloy was prepared by the extrusion (16:1) at 1505 K of appropriate amounts of blended Co-51.31 at % Al and Co-44.92 at % Al powders. After extrusion, oxide particles were present in the amount of 1 vol %, distributed as stringers parallel to the extrusion axis, and grains were equiaxed and roughly 11 μm in diameter.

2.2. Transmission electron microscopy

Transmission electron microscopy (TEM) was used to characterize the dislocation substructures of the Ni-48.2 at % Al and Co-49.3 at % Al alloys following extrusion. An electrical discharge machine was used to prepare 1 mm thick transverse sections from both extruded materials. After reducing the thickness of the sections to approximately 250 μm by grinding, the electrical discharge machine was used to cut out 3 mm diameter discs. The 3 mm discs were then thinned electrolytically at room temperature in an 8% perchloric-acetic acid solution. Thinned discs were examined in either a Philips EM400 or EM400ST microscope operated at 120 kV.

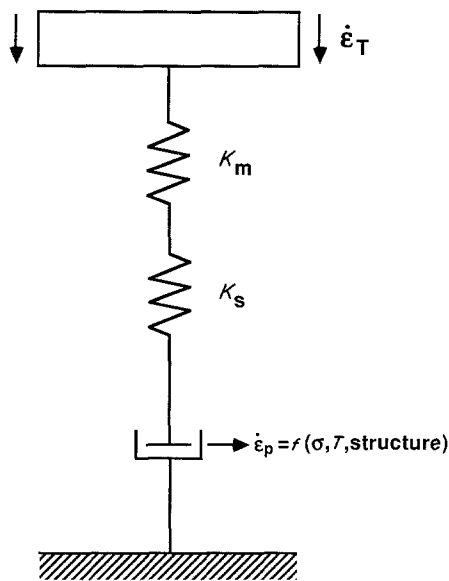


Figure 3 Schematic illustration of the elastic and plastic components of the testing system used. K_m and K_s are spring constants representative of elastic deformation in the testing machine and sample, respectively.

2.3. Compression testing

Constant total imposed true strain-rate compression tests were performed using an Instron 1125 electro-mechanical testing machine. A Hewlett-Packard data acquisition system was used to control the Instron and collect data during all tests. Samples were deformed between polished alumina platens with boron nitride used as the lubricant. Heating was accomplished with a split-shell type resistance furnace. Tests on NiAl were conducted over the temperature range 1100 to 1300 K at strain rates of either 10^{-4} or 10^{-3} sec^{-1} . Tests on CoAl were performed at slightly higher temperatures, 1200 to 1400 K, and the strain rate range was expanded to 5×10^{-6} to $1 \times 10^{-3} \text{ sec}^{-1}$.

2.4. Strain rate change tests

With the ability to control crosshead motion via the computer, it was possible to vary the crosshead speed during the course of a compression test either to maintain a constant total imposed true strain rate or to per-

form a strain rate change. Recently, Yaney *et al.* [15] developed a new technique involving strain rate changes for distinguishing between pure-metal and alloy-type of creep behaviour. These authors successfully used the technique to distinguish between pure-metal and alloy-type deformation behaviour, as exhibited by aluminium and the Class I solid-solution alloy Al-5.8at% Mg. In the remainder of this section, an abbreviated discussion of the strain rate change technique is given. For more detailed information regarding both the theory as well as the experimental details of the strain rate change technique, the reader should consult the paper by Yaney *et al.* [15].

In order to distinguish between pure-metal and alloy types of creep behaviour using the strain rate change technique, plastic strain rate is monitored as a function of stress during the deformation transient immediately following a strain rate change. The observed variation is then compared with the known variation of plastic strain rate with stress for steady-state deformation. A schematic illustration of the testing machine used in this investigation is shown in Fig. 3. As shown by Holbrook *et al.* [16], for a testing machine of this type the plastic strain rate is given by the equation

$$\dot{\epsilon}_{p1,\text{sample}} = \dot{\epsilon}_T - \dot{\epsilon}_{E1,\text{machine}} - \dot{\epsilon}_{E1,\text{sample}} \quad (1)$$

where $\dot{\epsilon}_{p1,\text{sample}}$ = the plastic strain rate of the sample, $\dot{\epsilon}_T$ = total strain rate imposed by the testing machine, $\dot{\epsilon}_{E1,\text{machine}}$ = the rate at which the testing machine deforms elastically, expressed as a strain rate, and $\dot{\epsilon}_{E1,\text{sample}}$ = the elastic strain rate of the sample. Equation 1 can equivalently be written as

$$\dot{\epsilon}_p = \frac{1}{L_p} \left(\dot{X} - \frac{\dot{P}}{K_m} - \frac{\dot{P}L_p^2}{EA_0L_0} \right) \quad (2)$$

where \dot{X} = crosshead speed, \dot{P} = loading rate, K_m = spring constant of the machine at the current load, E = Young's modulus of the sample, A_0 = initial area of the sample, L_0 = initial length of the sample, and L_p = unloaded length of the sample. Using Equation 2, plastic strain rate can be computed at any point during the experiment. Fig. 4 illustrates

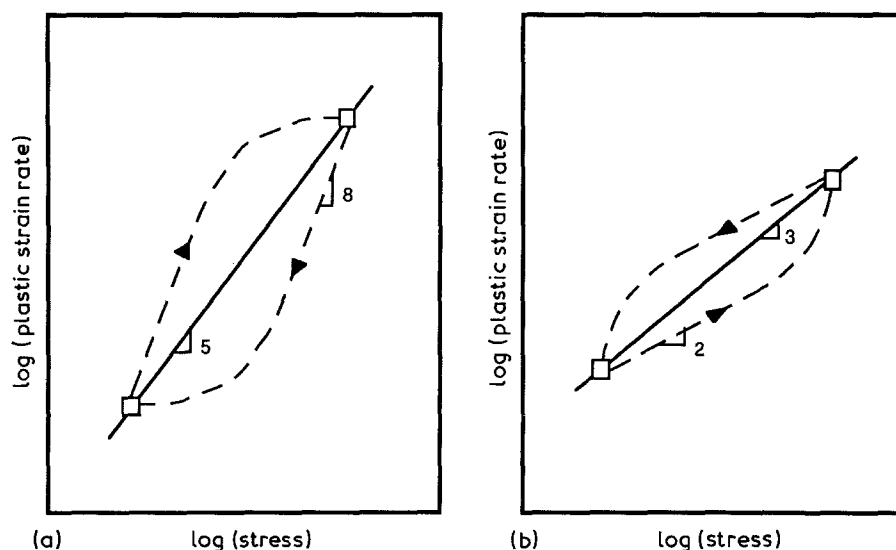


Figure 4 Double-logarithmic plot illustrating the variation of plastic strain rate with stress for (a) a pure metal and (b) an alloy-type material.

schematically how the variation in plastic strain rate with stress following a strain rate change can be used to distinguish between pure-metal and alloy-type creep behaviour. For a pure metal, deformation in the power-law regime is characterized by the formation of well-developed subgrains with a characteristic dimension, λ , which varies inversely with steady-state flow stress. Thus, for the case of a strain rate increase, the structure initially present after steady-state deformation at the lower strain rate is "softer" than the structure which is characteristic of steady-state flow at any higher stress value. As a result, the plastic strain rate during the transient is temporarily greater than the plastic strain rate predicted from steady-state data at the same stress. Only after sufficient microstructural refinement occurs is a return to steady-state behaviour observed.

For the case of a strain rate decrease in a pure metal, the structure formed by steady-state deformation at the initial high strain rate is "stronger" than the structure characteristic of steady-state flow at lower stresses. Thus, during the deformation transient, the plastic strain rate is less than that characteristic of steady-state deformation at the same stress. Significant microstructural softening is required before the plastic strain rate is no longer less than that predicted from steady-state data at the same stress.

Microstructure evolution in alloy-type materials differs considerably from microstructure evolution in pure metals. In alloy-type materials, subgrains generally do not form and under steady-state conditions, dislocations are present as a homogeneous distribution of loops. As a result, pure metals and alloy-type materials respond quite differently to changes in total imposed strain rate. For a strain rate increase in an alloy-type material, the dislocation density is initially lower than that characteristic of steady-state deformation at any higher stress value. Thus, the observed plastic strain rate is less than that predicted by the steady-state relation during the transient. Only after dislocation multiplication occurs is a return to steady-state behaviour observed. Analogously, for the case of a strain rate decrease, the dislocation density is initially too high. Until dislocation annihilation occurs, the plastic strain rate at a given stress is higher than that associated with steady-state deformation at that same stress.

It should be noted that no sudden change in plastic strain rate accompanies a change in total true strain rate in either pure metals or alloy-type materials if flow is thermally activated. The plastic strain rate depends only on the stress, temperature and structure, not on the stress rate. Since neither the stress or the structure change instantaneously and the temperature is held constant, no sudden change in plastic strain rate accompanies a change in imposed total strain rate under these conditions. Although the strain rates of the two elastic elements shown in Fig. 3 can change instantaneously, the strain rate of the dashpot, which represents plastic flow of the sample, cannot.

3. Results and discussion

3.1. Elevated-temperature tests of NiAl

Representative stress-strain curves obtained during

compression tests of the cast (Ni-49.3 at % Al) and extruded (Ni-48.2 at % Al) NiAl alloys tested at 1300 K are shown in Figs 5a and b, respectively. Note that the steady-state flow strengths of the two materials are virtually identical. As shown previously in Fig. 1, the strength of NiAl is not a strong function of composition at 1300 K. Thus differences in strength due to the 1% compositional variation between these two alloys is not expected at this temperature. With respect to the large difference in grain size between these two materials, a review of the literature reveals that the similarity in flow strength between the two materials is simply fortuitous and that the strength of NiAl actually does depend on grain size at 1300 K. The 1300 K flow strengths of several NiAl alloys with a variety of different grain sizes are plotted as a function of strain rate in Fig. 6 [4, 7, 18]. Alloys with grain sizes of 17, 18 and 225 μm exhibit almost identical flow strengths. However, an increase in grain size to 1000 μm is accompanied by a significant reduction in strength. Apparently any grain-boundary strengthening effects are overshadowed by softening mechanisms arising from grain-boundary diffusion. As the grain size is increased still further, such as in the as-cast alloy, an increase in strength is now observed. Apparently in this material, the total grain-boundary area is sufficiently small that softening due to enhanced diffusion is no longer significant.

Despite virtually identical steady-state behaviour, the cast and extruded NiAl alloys exhibit very different strain-hardening behaviours. As shown in Fig. 5b, the initial strain-hardening rate of the extruded material is quite high and steady-state conditions are achieved quickly (in the first 2 to 3% strain). The initial strain-hardening rate of the cast material is also high although, as can be seen in Fig. 5a, the strain-hardening rate decreases significantly after the first 2 to 3% strain but does not go to zero until 15 to 20% strain has been accumulated. This difference in strain-hardening behaviour may be related to differences in the mobile dislocation densities of the two types of NiAl prior to testing. As revealed by TEM, numerous dislocations are present in extruded NiAl prior to testing, presumably as a result of deformation during the extrusion process. In agreement with Whittenberger [4], an extensive subgrain network does not develop in NiAl during extrusion at 1505 K. However, deformation under the conditions used for testing in this investigation is apparently successful in forming such a network [4]. Although no TEM results were obtained, the as-cast NiAl should have a much lower dislocation density than the NiAl consolidated by extrusion. Thus, prior to testing, the mobile dislocation density should be highest in the extruded alloy. Work-hardening and subgrain formation should occur most rapidly (with less strain) in the extruded material.

Differences in grain size may also affect the strain-hardening behaviour of NiAl. During loading, grain boundaries are primary sources of dislocations [18, 19]. Since the grain-boundary area of the extruded material is much higher than that of the cast alloy, the dislocation density should increase more rapidly in the extruded material than in the coarse-grained casting.

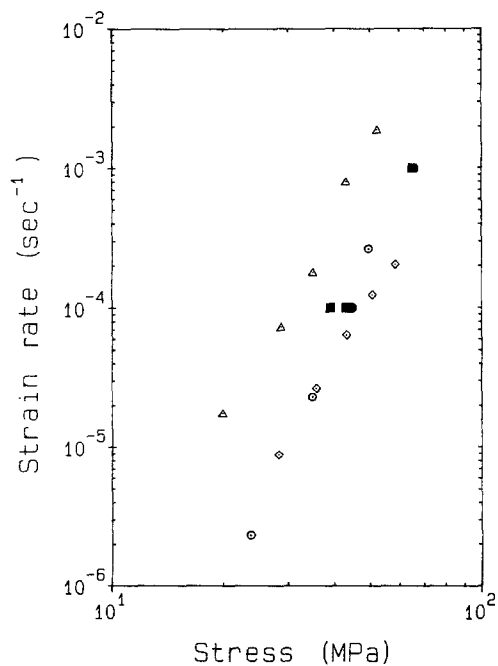
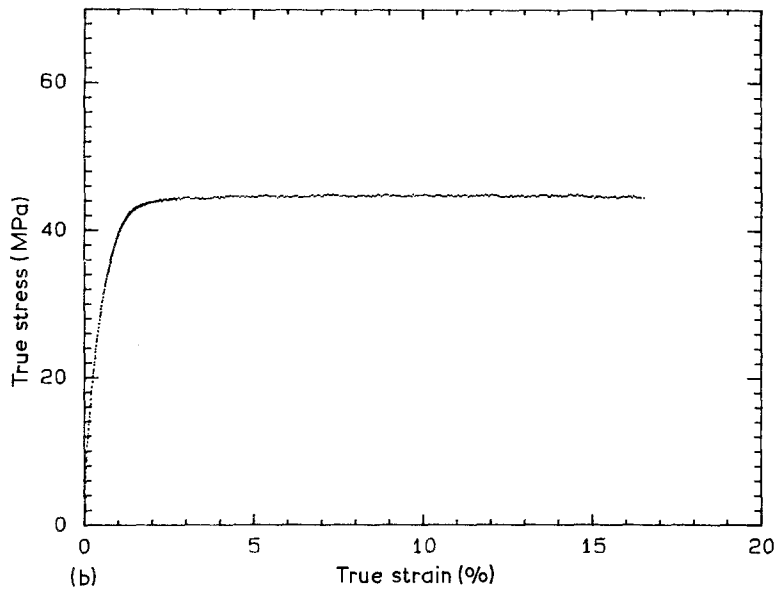
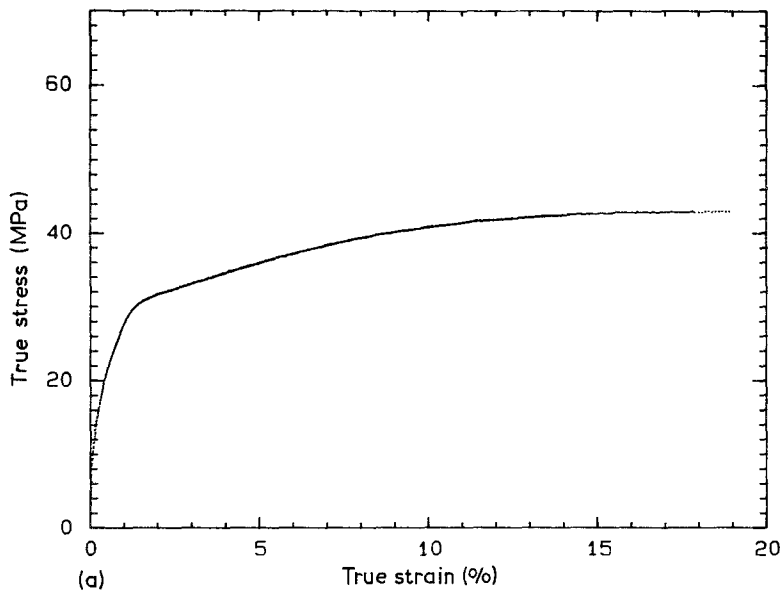


Figure 6 Comparison of steady-state flow data for NiAl tested at 1300 K. (■) 49.3% Al, as-cast (this work); (●) 48.2% Al, 18 μm grain size (this work); (○) 49.2% Al, 17 μm grain size [4]; (Δ) 50.4% Al, 1000 μm grain size [7]; (\diamond) 49.0% Al, 225 μm grain size [18].

Figure 5 Representative stress-strain curves for (a) as-cast Ni-49.3 at% Al and (b) as-extruded Ni-48.2 at% Al tested at 1300 K. Strain rate $1 \times 10^{-4} \text{ sec}^{-1}$.

Less strain should be required in the extruded material than in the cast alloy to form the subgrains characteristic of steady-state deformation in NiAl.

In order to study the ability of lattice friction to reduce dislocation mobility in NiAl, strain rate change tests were performed. The results of strain rate increase and decrease tests on the cast alloy at 1300 K are shown in Figs 7a and b, respectively. As discussed in Section 2, these transients are indicative of pure-metal type behaviour and thus are consistent with the observation by a number of investigators [4, 12, 17] of the formation of subgrains under similar test conditions. It should be pointed out that the apparent lack of strain-rate continuity immediately following the increase in strain rate (Fig. 7a) is an artifact of the specific test technique used and does not reflect true material behaviour. As discussed elsewhere [15], the apparent lack of strain-rate continuity immediately following an increase in strain rate is related to the difficulties associated with accurately determining K_m . A complete discussion of this problem, including methods for avoiding it in the future, are given by Yaney *et al.* [15]. Despite the inaccuracies in plastic strain rate measurements immediately following

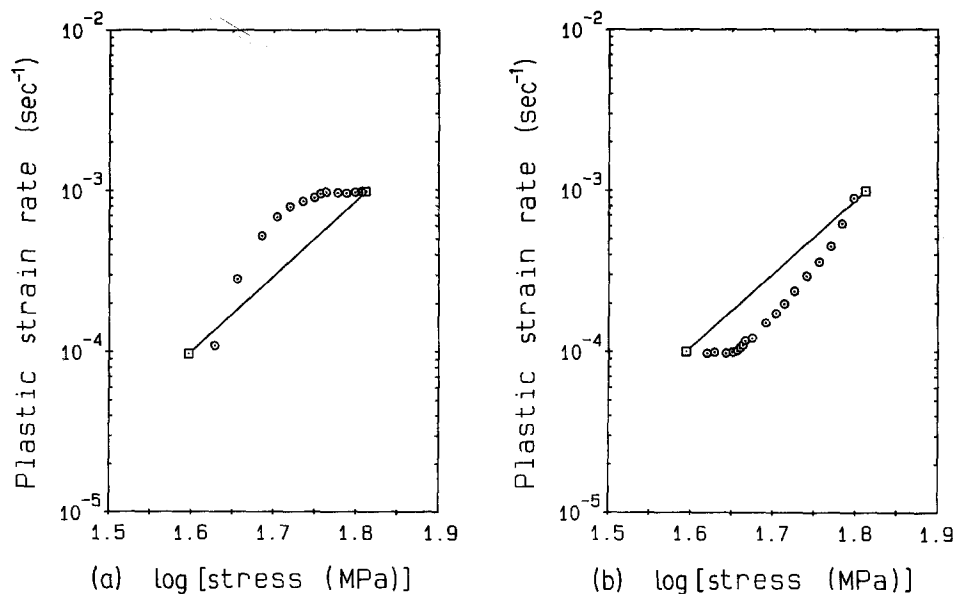


Figure 7 Double-logarithmic plots of plastic strain rate against stress for (a) a strain rate increase and (b) a strain rate decrease in cast Ni-49.3 at % Al tested at 1300 K; (□) steady-state behaviour, (○) transient behaviour.

increases in strain rate, a pure-metal type of transient was also observed in the cast material at 1100 K. Thus, lattice friction does not limit the motion of dislocations in NiAl at temperatures between 1100 and 1300 K. Pure-metal type behaviour is observed, indicating that dislocation substructure is controlling deformation.

With regard to extruded NiAl, a pure-metal type of transient was observed at 1300 K. However, as can be seen in Fig. 8, the transient is not as dramatic in the extruded alloy as in the cast alloy. Apparently, recovery processes occur most rapidly in the material prepared by extrusion. In order to understand the difference in recovery rates between the two materials it is necessary to note, once again, that these two materials have drastically different grain sizes. The fine-grained alloy produced by extrusion has more grain-boundary area per unit volume than its coarse-grained counterpart. Since grain boundaries are sources of dislocations [18,

19], more dislocations are generated per given increment of strain, following a strain rate increase, in extruded NiAl than in the cast NiAl. Substructural changes occur more rapidly in the extruded material. Hence, the deviations from steady-state behaviour observed following a strain rate increase are smallest in the NiAl prepared by extrusion.

3.2. Elevated-temperature tests of CoAl

As discussed in Section 2, all tests on CoAl were performed on a 49.3 at % Al alloy prepared by the extrusion (16:1) of gas-atomized powders at 1505 K. A TEM micrograph of the dislocation substructure developed in CoAl during extrusion is shown in Fig. 9. In direct contrast to NiAl extruded at the same temperature using the same reduction ratio, well-developed subgrains are present. A typical stress-strain curve obtained during compression testing of CoAl at 1400 K is shown in Fig. 10. The initial work-hardening rate is high and steady-state flow conditions are attained after 2 to 3% strain. Note that the stress-strain response of CoAl at this temperature is quite similar to that of NiAl at 1300 K. Fig. 11 reveals that at 1300 K a maximum flow stress is reached after 2 to 3% accumulated strain. Steady-state conditions are never attained. Instead, flow softening is observed. Fig. 12 shows that at 1200 K, 5 to 8% strain is required to reach a maximum in flow stress. Strain softening, more severe than at 1300 K, is readily observed. Steady-state flow does not occur.

In attempting to determine the cause of flow softening in CoAl at 1200 and 1300 K, it was noted that NiAl, produced under identical conditions, did not show flow softening. However, NiAl (unlike CoAl) did not develop a network of subgrains during extrusion. Despite the high extrusion temperature, the subgrain network formed during consolidation of CoAl is likely to be fairly stable during lower-temperature testing as a result of the relatively high strain rates associated with the extrusion process. Recall that although typical strain rates for extrusion range from

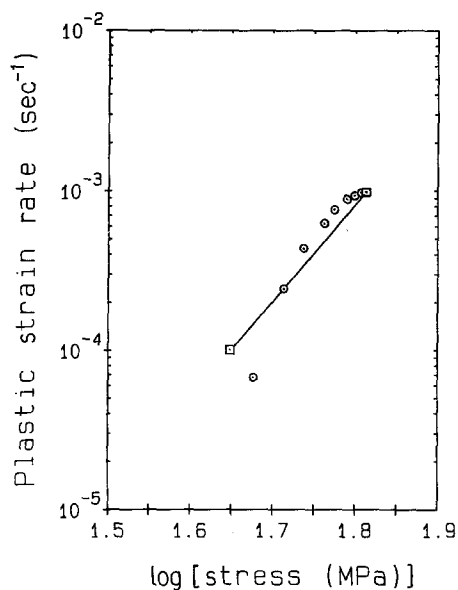


Figure 8 Double-logarithmic plot of plastic strain rate against stress for a strain rate increase in extruded Ni-48.2 at % Al tested at 1300 K.

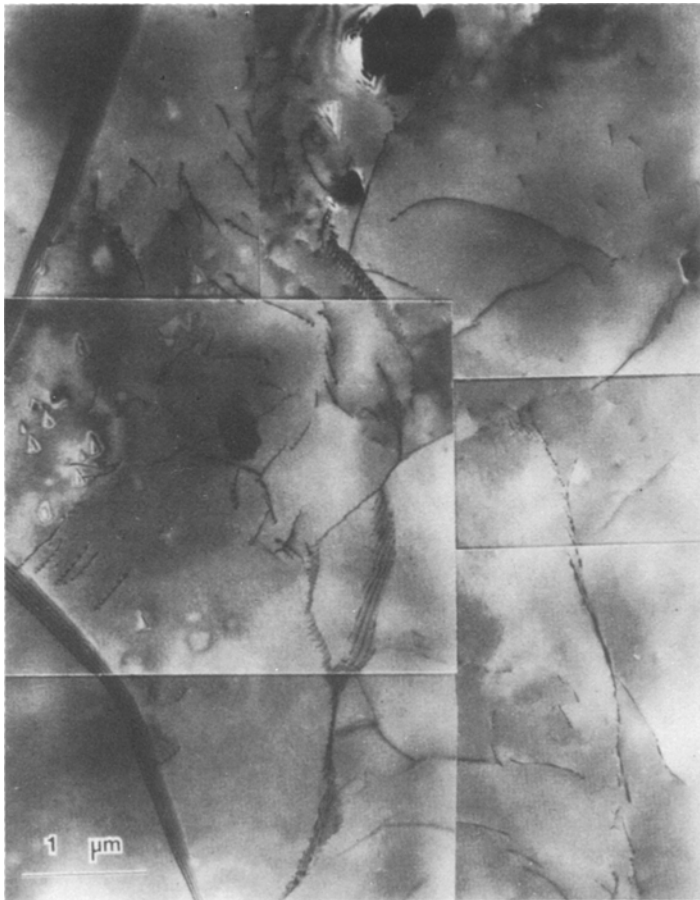


Figure 9 TEM micrograph of Co-49.3 at % Al showing dislocation substructure developed during extrusion.

1 to 10 sec^{-1} , the strain rates used during testing never exceeded 10^{-3} sec^{-1} . Thus, it is postulated that flow softening in CoAl at 1200 and 1300 K is due to the gradual replacement of the substructure formed during extrusion by a substructure characteristic of lower-temperature deformation. In other words, as the test temperature is lowered, the subgrain network formed during extrusion at 1505 K becomes increasingly more difficult to replace. Diffusion becomes more sluggish at lower test temperatures. Hence, the lower the test temperature, the more deformation and/or time at temperature required to break up the substructure formed during extrusion and replace it with

the structure characteristic of steady-state deformation at the lower test temperature.

In order to determine the validity of the ideas just outlined, it was necessary to test CoAl in which the subgrain network formed during extrusion at 1505 K was no longer present. Two techniques for breaking up the initial subgrain network were employed. The first involved annealing the extruded material for 2 h at 1400 K prior to testing. In the second technique, extruded material was deformed 10% at 1400 K prior to testing at a lower temperature. TEM of samples annealed at 1400 K for 2.5 h revealed that annealing is reasonably successful in breaking up the subgrains

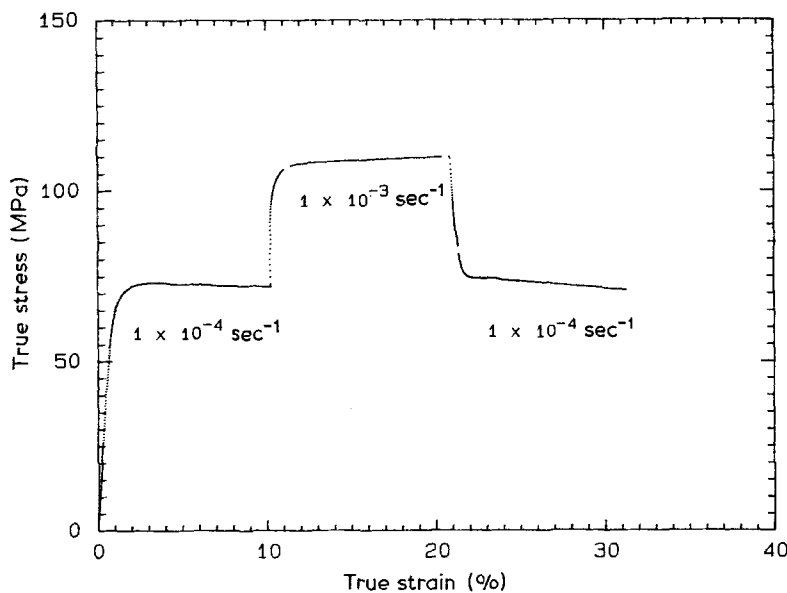


Figure 10 Representative stress-strain curve for extruded Co-49.3 at % Al tested at 1400 K. Strain rate changes are indicated.

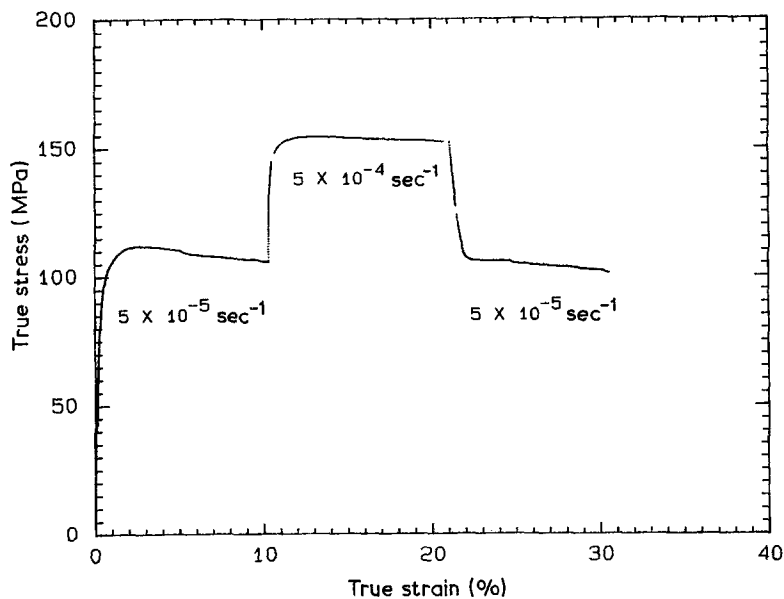


Figure 11 Representative stress-strain curve for extruded Co-49.3 at % Al tested at 1300 K. Strain rate changes are indicated.

formed during extrusion. The results of compression tests performed on annealed CoAl are shown in Fig. 13. Pre-straining at 1400 K produced similar changes in flow behaviour. As a result of pre-treatment, the initial flow stress of CoAl is lowered approximately 20% and flow softening is significantly reduced. Thus, not only is the subgrain network formed during extrusion responsible for flow softening at 1200 K, it produces significant strengthening during the initial stages of testing at this temperature as well.

With regard to the influence of prior substructure on deformation at 1300 and 1400 K, it should be remembered that the severity of flow softening decreases with increasing test temperature. In fact, at 1400 K steady-state behaviour is observed; apparently the annealing during heat-up and deformation during loading are sufficient to break up the substructure formed during extrusion. Although not as severe as at 1200 K, Fig. 11 shows that some strain softening does occur during testing at 1300 K. Apparently annealing during heat-up and deformation during loading are only partially successful at this lower temperature in breaking up the substructure formed during extrusion.

As was done for NiAl, strain rate change tests were also performed on CoAl. Log-log plots of plastic strain rate against stress following strain rate increments in Co-49.3 at % Al at 1400, 1300 and 1200 K are shown in Figs 14a to c, respectively. The test at 1200 K was performed on a sample that had been annealed for 2 h at 1400 K prior to testing. At 1400 K, Fig. 14a shows a pure-metal type of transient response. As was observed in extruded NiAl, the transient is not dramatic. At 1300 K, a transient response is no longer resolvable. However, once the test temperature is lowered to 1200 K, an alloy-type transient is observed. Fig. 14 clearly shows that there is a transition from pure-metal to alloy-type deformation behaviour in Co-49.3 at % Al as the test temperature is lowered from 1400 to 1200 K. Thus, the deformation characteristics of CoAl differ considerably from those of NiAl. NiAl exhibits pure-metal type behaviour at 1200 K. CoAl, on the other hand, exhibits alloy-type deformation behaviour at this temperature. Apparently, lattice friction effects are able to limit the mobility of dislocations at a much higher temperature in CoAl than in NiAl. Thus, it is not surprising that

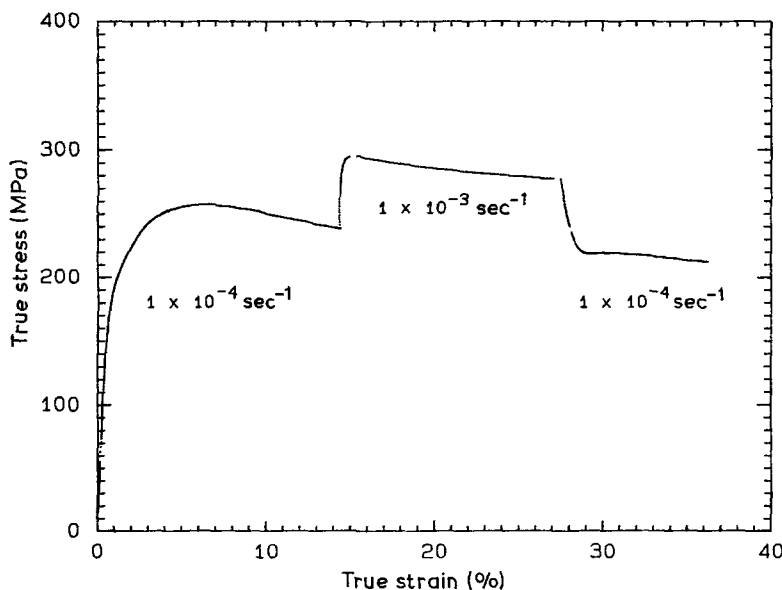


Figure 12 Representative stress-strain curve for extruded Co-49.3 at % Al tested at 1200 K. Strain rate changes are indicated.

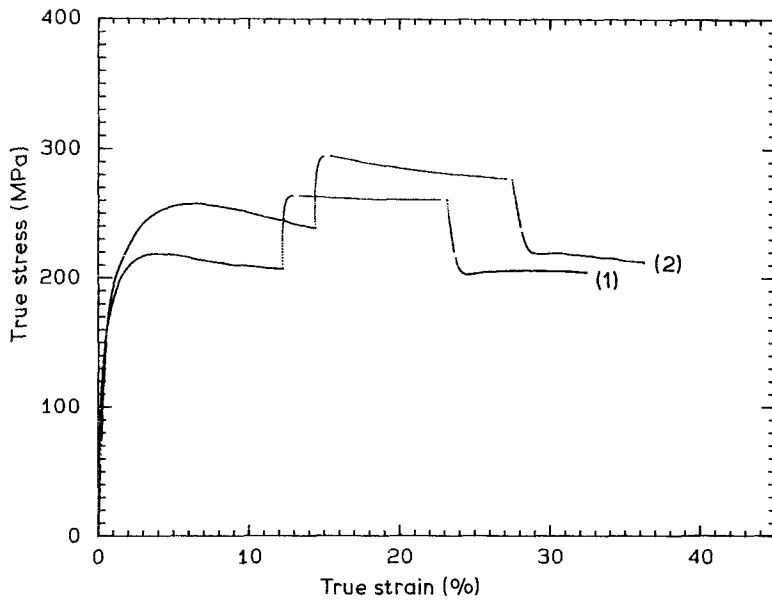


Figure 13 (1) Representative stress-strain curve for extruded Co-49.4at% Al annealed for 2 h at 1400 K prior to testing at 1200 K. (2) Test of the as-extruded material shown for comparison. First strain rate: $1 \times 10^{-4} \text{sec}^{-1}$, second strain rate: $1 \times 10^{-3} \text{sec}^{-1}$, third strain rate: $1 \times 10^{-4} \text{sec}^{-1}$.

the elevated-temperature strength of CoAl is noticeably superior to that of NiAl.

Although the strain rate change test was successful in detecting the transition from pure-metal to alloy-type behaviour in CoAl, difficulties were sometimes

encountered in detecting deformation transients in the extruded material, especially following decrements in strain rate. As shown in Fig. 14a, a pure-metal type deformation transient, although not dramatic, is resolvable in CoAl following an increment in strain rate at 1400 K. However, when the strain rate is reduced no deviation from steady-state behaviour can be detected. Apparently, as in extruded NiAl, recovery occurs rapidly in fine-grained CoAl. In large-grained materials such as pure aluminium [15] or cast NiAl, deformation transients are easily resolved even following decrements in strain rate. Thus in fine-grained CoAl, grain boundaries act as sources for dislocations following increments in strain rate and act as sinks for dislocations following decrements in strain rate. The difficulty in detecting transient behaviour following decreases in strain rate may simply be related to the

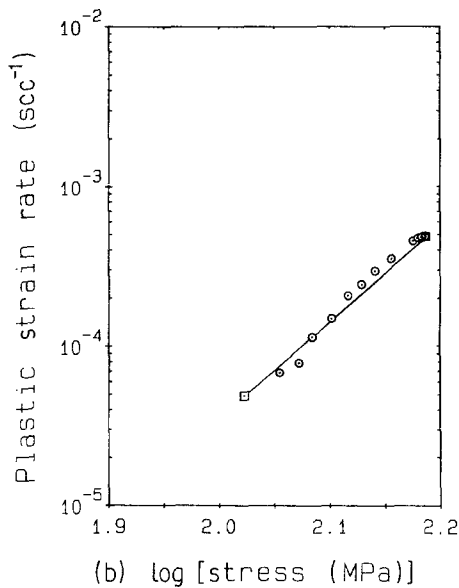
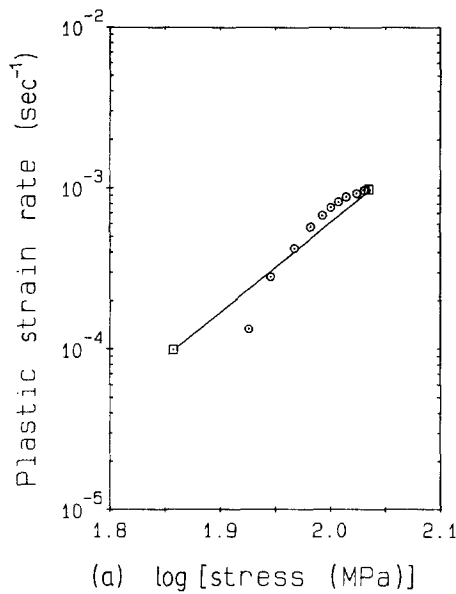
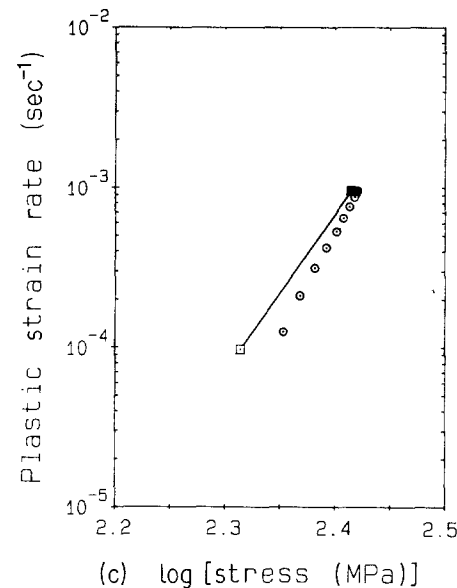


Figure 14 Double-logarithmic plot of plastic strain rate against stress following a strain rate increase in Co-49.3 at % Al tested at (a) 1400 K, (b) 1300 K and (c) 1200 K. Tests (a) and (b) performed on as-extruded material. Test (c) performed on material that had been annealed for 2 h at 1400 K. (□) Steady-state behaviour, (○) transient behaviour.



fact that the stress changes more slowly following a decrease in strain rate than it does following an increase in strain rate of the same magnitude. As a result, following a reduction in strain rate, the system may never be perturbed far enough from steady state that recovery processes cannot keep up.

At 1300 K, no clear transient response is resolvable following either an increase or decrease in strain rate. Once again, it is expected that the large grain-boundary area of the fine-grained CoAl is speeding recovery. However, a clear transient response is also not expected at this temperature since CoAl undergoes a transition from pure-metal to alloy-type behaviour between 1400 and 1200 K.

At 1200 K, strain-rate-increase tests of samples annealed or deformed at 1400 K prior to testing clearly show that deformation in CoAl at this temperature proceeds by an alloy-type mechanism. Although difficult to resolve, strain rate decrease tests also show an alloy-type response. As seen in strain rate change tests of coarse-grained Al-5.8 at % Mg [15], deformation transients in alloy-type materials are difficult to resolve even under the best of circumstances. When CoAl is tested at 1200 K without prior annealing or deformation at 1400 K, large amounts of flow softening are superimposed upon the alloy-type deformation transient which is inherently difficult to resolve. Thus, it is not surprising that alloy-type behaviour is not discernible in CoAl that still contains the substructure formed during extrusion.

4. Summary

A strain rate change technique developed previously to distinguish between pure-metal and alloy-type creep behaviour was used to study the elevated-temperature deformation behaviour of the intermetallic compounds NiAl and CoAl. NiAl exhibits pure-metal type behaviour over the temperature range 1100 to 1300 K. CoAl, on the other hand, undergoes a transition from pure-metal to alloy-type deformation behaviour upon lowering the test temperature from 1400 to 1200 K. Lattice friction effects appear to limit the mobility of dislocations at a much higher temperature in CoAl than in NiAl. The difference in strength between NiAl and CoAl may therefore be related to a greater lattice friction strengthening effect in CoAl than in NiAl.

Acknowledgements

This work was sponsored by the NASA Lewis Research Center under Grant No. NASA NAG 3-248. The authors thank Dr J. D. Whittenberger of the NASA Lewis Research Center for initiating this project and for providing all the extruded materials used in this study. The assistance of Dr C. T. Liu of the Oak Ridge National Laboratory in providing cast NiAl is gratefully acknowledged.

References

1. "Metals Handbook", Vol. 8 (8th Edn) (American Society for Metals, 1964) pp. 258, 262.
2. M. R. HARMOUCHE and A. WOLFENDEN, *J. Testing Eval.* **13** (1985) 424.
3. M. J. COOPER, *Phil. Mag.* **89** (1963) 805.
4. J. D. WHITTENBERGER, *J. Mater. Sci.* **22** (1987) 394.
5. *Idem*, *Mater. Sci. Eng.* **73** (1985) 87.
6. L. A. HOCKING, P. R. STRUTT and R. A. DODD, *J. Inst. Metals* **99** (1971) 98.
7. R. R. VANDERVOORT, A. K. MUKHERJEE and J. E. DORN, *Trans. ASM* **59** (1966) 930.
8. J. H. WESTBROOK, *J. Electrochem. Soc.* **103** (1956) 54.
9. N. RUSOVIC and H. WARLIMONT, *Phys. Status Solidi* **53** (1979) 283.
10. D. L. YANEY, A. R. PELTON and W. D. NIX, *J. Mater. Sci.* **21** (1986) 2083.
11. A. BALL and R. E. SMALLMAN, *Acta Metall.* **14** (1966) 1349.
12. J. BEVK, R. A. DODD and P. R. STRUTT, *Metall. Trans.* **4** (1973) 159.
13. S. SCHAFER, *Phys. Status Solidi* **19** (1967) 297.
14. A. R. CHAUDHURI, J. R. PATEL and L. G. RUBIN, *J. Appl. Phys.* **33** (1962) 2736.
15. D. L. YANEY, J. C. GIBELING and W. D. NIX, *Acta Metall.* **35** (1987) 1391.
16. J. H. HOLBROOK, J. C. SWEARENGEN and R. W. ROHDE, ASTM STP 765 (American Society for Testing and Materials, Philadelphia, 1982) p. 80.
17. W. J. YANG and R. A. DODD, *Met. Sci.* **7** (1973) 41.
18. P. J. WORTHINGTON and E. SMITH, *Acta Metall.* **12** (1964) 1277.
19. K. TANGRI and K. N. TANDON, in "Grain Boundaries in Engineering Materials", edited by J. L. Walter, J. H. Westbrook and D. A. Woodford (Claitor, Baton Rouge, 1975) p. 327.

Received 23 April
and accepted 6 July 1987